Proceedings World Geothermal Congress 2020+1
Reykjavik, Iceland, April - October 2021

On Study of Mineral Scaling of Brine Reinjection Using Thermo-hydro-chemical Coupled Simulation

Jingyi Chen, Tianfu Xu, Zhenjiao Jiang, Bo Feng

Key Laboratory of Groundwater Resources and Environment, Ministry of Education, Jilin University, Changchun, 130021, China

jychen18@mails.jlu.edu.cn

Keywords: Reactive transport modeling; Mineral scaling; Injection; Water-rock interaction.

ABSTRACT

Tail water reinjection is widely used in geothermal energy production system, to maintain the continuous fluid flow. However, geothermal water is often type of brine with high dissolved salts, injection of high salinity cold geothermal fluid may cause strong chemical reactions, leading to scaling in the reservoir. Subsequently, porosity and permeability in the reservoir and injection capacity of the system would be weakened significantly. Therefore, scaling is one of the key problems that restrict the sustainable utilization of geothermal energy. This study numerically investigated the mechanism of chemical scaling in the reservoir of Soultz-sous-forets geothermal field. It was found that calcite and quartz are the major minerals causing scaling. We thus proposed to reduce scaling by diluting geothermal water and adding mud acid, and found that both can improve the porosity of the reservoir and the performance of the geothermal system.

1. INTRODUCTION

An enhanced geothermal system (EGS) is artificially formed by creating fractures in hot dry rock to enhance heat energy production (Tester, Anderson et al. 2007, Kushnir, Heap et al. 2018). The Soultz-sous-forets site in France is one of the successful EGS sites, which began generating electricity in 2008. Three wells (GPK3 as injection well, GPK2 and GPK4 as production wells) were drilled to a maximum depth of 5000 m in the crystalline rock (Bächler and Kohl 2005, Dezayes, Genter et al. 2010, Portier and Vuataz 2010). However, the salinity of geothermal fluid can be as high as 100 g/L, which would cause scaling problems in the geothermal plant and reservoir. In addition, chemical stimulation has a strong local effect, which leads to precipitation of secondary clay and silicon and carbonate minerals to seal the natural crack (André, Rabemanana et al. 2005, Portier, Hinderer et al. 2018). It was reported in the Soultz-sous-forets geothermal power plant that pipe diameter has been reduced significantly due to the scaling accompanied with the geothermal fluid circulation in the system. This subsequently blocked the transport of heat and fluid (Nitschke, Scheiber et al. 2014). Acid treatments have been successfully applied in many cases to increase geothermal wells production rates to commercial levels (Entingh 1999, André, Spycher et al. 2008). Sandrine Portier et al. (2009) demonstrated that acidification treatment can improve reservoir porosity and permeability, especially near injection well (Portier and Vuataz). Laurent André et al. (2009) concluded that injection of diluted brines combined with periodically reverse circulation in the reservoir could help maintain the long-term productivity of fractured reservoirs in granitic rocks (André, Rabemanana et al. 2006).

This study aims to explore the scaling processes in the reservoir, and optimize the methods to prevent scaling and improve the porosity and permeability of the reservoir, and then injection rate.

2. NUMERICAL MODELING APPROACH

The simulator used in this study is TOUGHREACT, which is well-accepted multi-phase reactive transport program (Xu, Spycher et al. 2011). Changes in porosity are calculated according to changes in mineral volume fraction, Changes in permeability are expressed by Kozeny-Carman model (Bear 1972):

$$\frac{k}{k_0} = \left(\frac{\phi}{\phi_0}\right)^3 \left(\frac{1-\phi_0}{1-\phi}\right)^2 \tag{1}$$

where ϕ is the porosity, k is the permeability (m^2), and subscripts 0 denote initial values of each variable.

The kinetic reaction processes between fluid and minerals is controlled by (Lasaga 1984):

$$r = A_r k_{25} \exp\left[\frac{-E_a}{R}\left(\frac{1}{T} - \frac{1}{298.15}\right)\right]\left(1 - \frac{Q}{K}\right) \tag{2}$$

where r refers to the reaction rate, A_r is the reactive surface area, K_{25} refers to the reaction rate constant at 25°C, E_a is the activation energy, T and R are the temperature (K) and ideal gas constant, Q and K refer to the ion activity product and equilibrium constant of a specific mineral reaction.

The parameters in the kinetic rate expression used are shown in Table 1. For most minerals, a reaction order n (acid catalyzed) greater than zero represents mineral dissolution, while n = 0 (no catalysis) represents precipitation (Xu and Pruess 2004).

Table 1 The reaction parameters for primary minerals and the secondary minerals in the geothermal reservoir.

Mineral	Chemical formula	$k_{n,25}$ ($molm^{-2}\ s^{-1}$)	n	E_a (kJ/mol)	Specific reactive area (cm^2/g)
Primary minerals					
Calcite	$CaCO_3$	Equilibrium		-	-
Quartz	SiO_2	1.0e-14	0	87.50	9.8
K-feldspar	$KAlSi_3O_8$	1.0e-12	0	57.78	9.8
		3.5e-10	0.4	51.83	9.8
Illite	$K_{0.6}Mg_{0.25}Al_{1.8}(Al_{0.5}Si_{3.5}O_{10})(OH)_2$	1.0e-13	0	62.76	151.6
		4.4 e-12	0.17	62.76	62.76
Secondary minerals					
Chlorite	$Mg_{2.5}Fe_{2.5}Al_2Si_3O_{10}(OH)_8$	3.0e-13		88.00	9.8
Ca-smectite	$Ca_{0.145}Mg_{0.26}Al_{1.77}Si_{3.97}O_{10}(OH)_2$	1.7e-13		35.00	151.6
Dolomite	$CaMg(CO_3)_2$	3.0e-8		52.20	9.8
Kaolinite	$Al_2Si_2O_5(OH)_4$	6.9e-14		22.20	151.6

3. MODEL SETUP

Conceptual model considers a one-dimensional flow tube with a length of 600 m between injection and production wells. The domain was divided into 76 grid blocks, to reveal mechanism of chemical reactions between injected fluid and reservoir rocks in the Soultz geothermal field (Fig. 1).

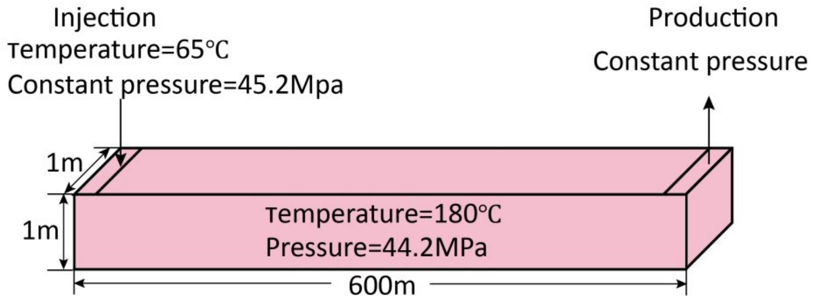

Figure 1: Boundary conditions assigned on the one-dimensional model domain.

An initial temperature of 180 °C and a hydrostatic pressure of 44.2 MPa were defined in the model domain following the conditions at the depth of 4500 m in the reservoir. Water was initially injected into the modelled zone at a rate of 1.76×10^{-2} L/s with a temperature of 65 °C. Water was extracted from the domain by defining a constant pressure of 45.2 MPa near the injection well of 1 m. The thermophysical parameters considered in the simulation were listed in Table 2.

Table 2 Thermophysical parameters controlling fluid and heat transport in the Soultz-sous-forets.

Parameter	Value
Density of granite	2650 kg/m^3
Density of geothermal fluid	1000 kg/m^3
Thermal conductivity in granite	2.90 W/(m·°C)
Thermal conductivity of geothermal fluid	0.62 W/(m·°C)
Heat capacity of granite	838 J/(kg·°C)
Heat capacity of geothermal fluid	4200 J/(kg·°C)
porosity	0.1
permeability	$2.0 \times 10^{-12}\ m^2$

The initial chemical composition were defined according to the measurements on the water samples collected from 3500 m in in GPK2 well, which reached an equilibrium state with mineral components under the condition of 180 °C. The injected water is type of Cl-Na·Ca (Genter, Evans et al. 2010) (considered as the base case), which is diluted by a factor of 3 in case 2 and mixed with HF with a concentration of 3% in case 3 (Table 3).

Table 3 The chemical component of initial water and injection water.

Fluid	Initial water	Hydrochemical water	Diluted water	Acidic water
T (°C)	180°C	65°C	65°C	65°C
pH	5.0	5.03	5.50	1.82
K^+ (mol/L)	1.022 x 0^{-1}	7.179 x10^{-2}	2.393x10^{-2}	7.179 x10^{-2}
Na^+ (mol/L)	1.213	0.9956	0.4404	0.9956
Ca^{2+} (mol/L)	1.250 x10^{-1}	0.1525	6.067 x10^{-2}	0.1525
Mg^{2+} (mol/L)	4.282 x10^{-2}	4.416 x10^{-3}	1.536 x10^{-3}	4.416 x10^{-3}
Al^{3+} (mol/L)	5.642 x10^{-7}	5.656x10^{-9}	1.885x10^{-9}	5.656x10^{-9}
TFe (mol/L)	7.680 x10^{-9}	1.491x10^{-6}	4.970 x10^{-7}	1.491x10^{-6}
Cl^- (mol/L)	1.720	1.388	0.573	1.388
SO_4^{2-} (mol/L)	2.020x10^{-3}	1.635x10^{-3}	6.733 x10^{-4}	1.635x10^{-3}
HCO_3^- (mol/L)	1.023x10^{-3}	7.795x10^{-3}	2.500 x10^{-3}	7.795x10^{-3}
f^- (mol/L)	0.1516E-09	0.1516E-09	0.1516E-09	0.1516E-01
SiO_2 (mol/L)	3.318x10^{-3}	4.129x10^{-3}	1.376 x10^{-3}	4.129x10^{-3}

The mineralogical composition of Soultz granite between two wells (GPK2 and GPK3), and minerals accounted for in the numerical modeling were given in Table 4 (Jacquot 2000).

Table 4 Initial volume fractions of minerals used in simulation.

Mineral	Chemical formula	Volume fraction vol.%
Primary minerals		
Calcite	$CaCO_3$	3.30
Quartz	SiO_2	40.9
K-feldspar	$KAlSi_3O_8$	13.9
Illite	$K_{0.6}Mg_{0.25}Al_{1.8}(Al_{0.5}Si_{3.5}O_{10})(OH)_2$	24.6
Secondary minerals		
Chlorite	$Mg_{2.5}Fe_{2.5}Al_2Si_3O_{10}(OH)_8$	0
Ca-smectite	$Ca_{0.145}Mg_{0.26}Al_{1.77}Si_{3.97}O_{10}(OH)_2$	0
Dolomite	$CaMg(CO_3)_2$	0
Kaolinite	$Al_2Si_2O_5(OH)_4$	0

4. RESULTS

4.1 Scaling mechanism in the reservoir

The fluid circulation inside the rock mass is carried out in the hydrothermal alteration granite, and the precipitation and dissolution laws of each mineral in 10 years are simulated. The injection temperature is 65 °C, and the rock matrix can buffer the change of temperature. Circulation of colder fluids through the fractured zone disturbs the chemical equilibrium of the rock–brine system, resulting in mineral precipitation and/or dissolution. The low-temperature water gradually diffuses to the mining section, reducing the temperature continuously. It is estimated that the production temperature drops to 160 °C in 10 years. The relative porosity decreases by 4.5% in 10 years in the injection section, and slightly decreases near the production section (Fig. 2).

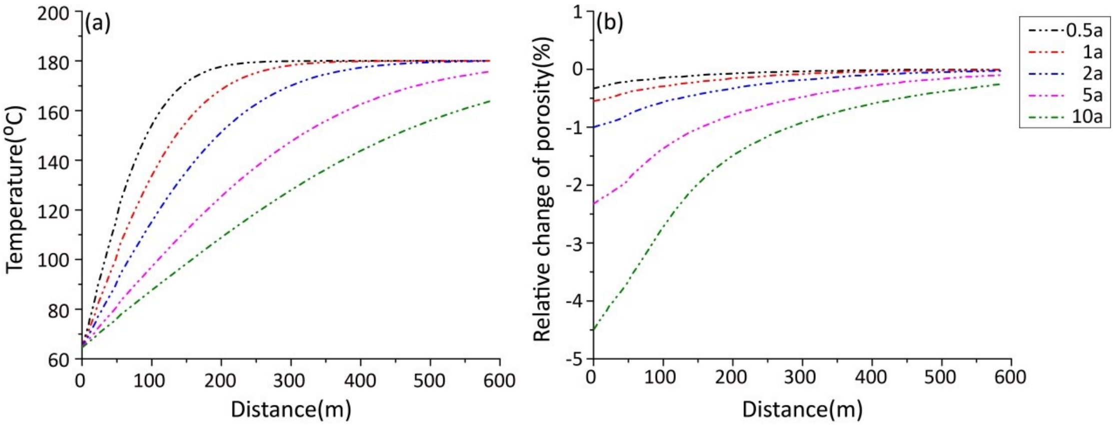

Figure 2: Distribution of temperature and relative change of porosity along the flow path in the model domain.

Ca^{2+} of injection hydrochemical water in granite is in a supersaturated state, which leads to the precipitation near the injection well. The relative change of porosity is mainly induced by the precipitation of calcite. The change of calcite increases by 0.45 in 10 years in the injection section. The reaction of calcite is an order of magnitude larger than the reaction of quartz with rock. Precipitation of quartz decreases along the flow path, with a maximum variation of 0.025 in abundance over 10 years. However, at the position near the production well, the decrease in temperature leads to dissolution of quartz. K-feldspar has a weak precipitation near the injection section, however, it dissolves at the production section (Fig. 3).

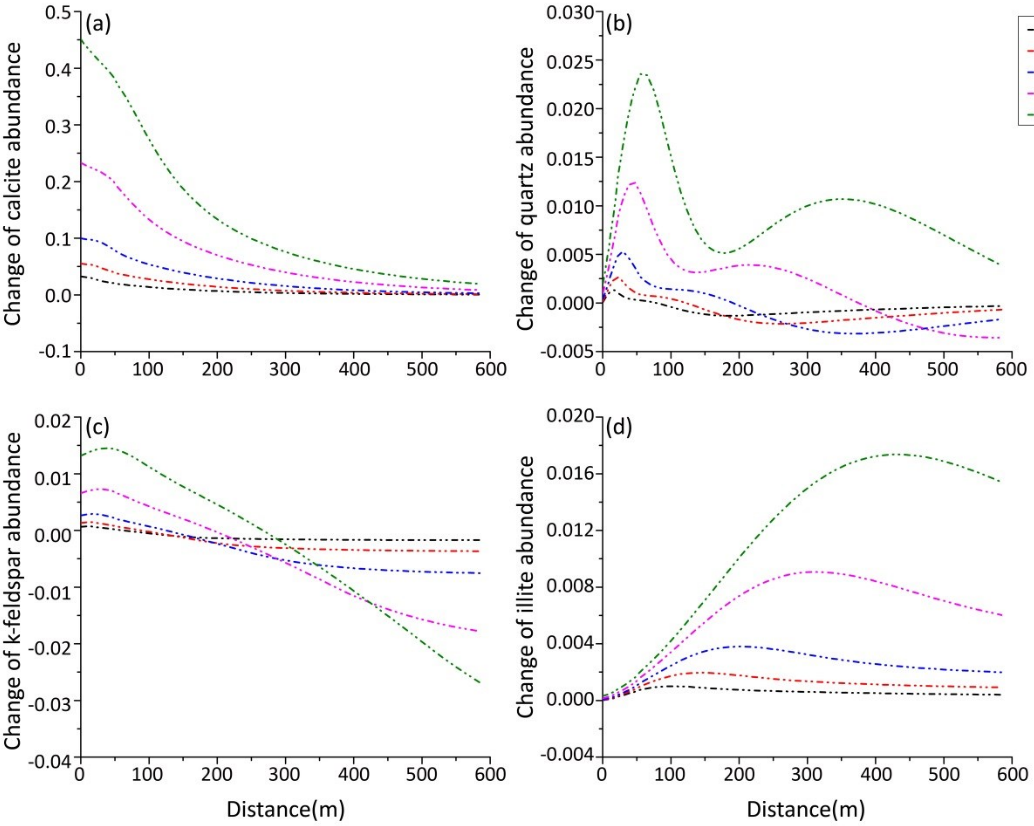

Figure 3: Variation of abundance of (a) calcite, (b) quartz, (c) k-feldspar, (d) illite along the flow path.

4.2 Effects of dilution and acidification

Dilution injection can promote mineral dissolution near the injection well. This method reduces the precipitation of calcite. However, diluted water reduces the ionic strength of the injected water, which may cause swelling of the clay in the granite. The significant precipitation of illite was observed, which reduces porosity in reservoir (Fig 4b). The percentage of fresh water in the injection fluid should be accurately determined. The acid injection dissolved a large amount of calcite and the change of other minerals abundance was weak compared with the change of calcite abundance (Fig. 4).

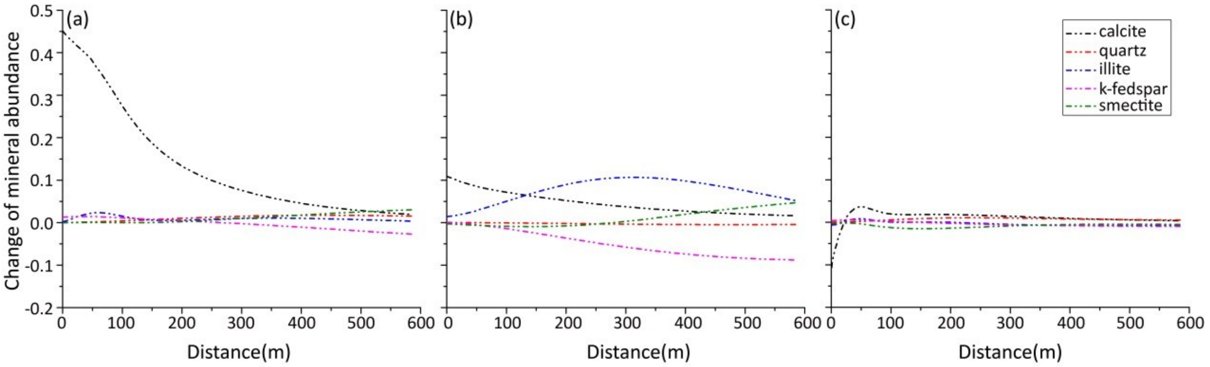

Figure 4: Variation of minerals along the flow path under (a) injection of hydrochemical water, (b) injection of diluted water, and (c) injection of acidic water.

Compared the three schemes, it was found that the acidic case has the most obvious effect on reservoir improvement, which improved the porosity and permeability of the reservoir and lead to the increase of the injection rate. The injection rate was reduced from 0.019 kg/s to 0.015 kg/s in 10 years, meanwhile, relative change of porosity increased 1.5% near the injection well (Fig. 5).

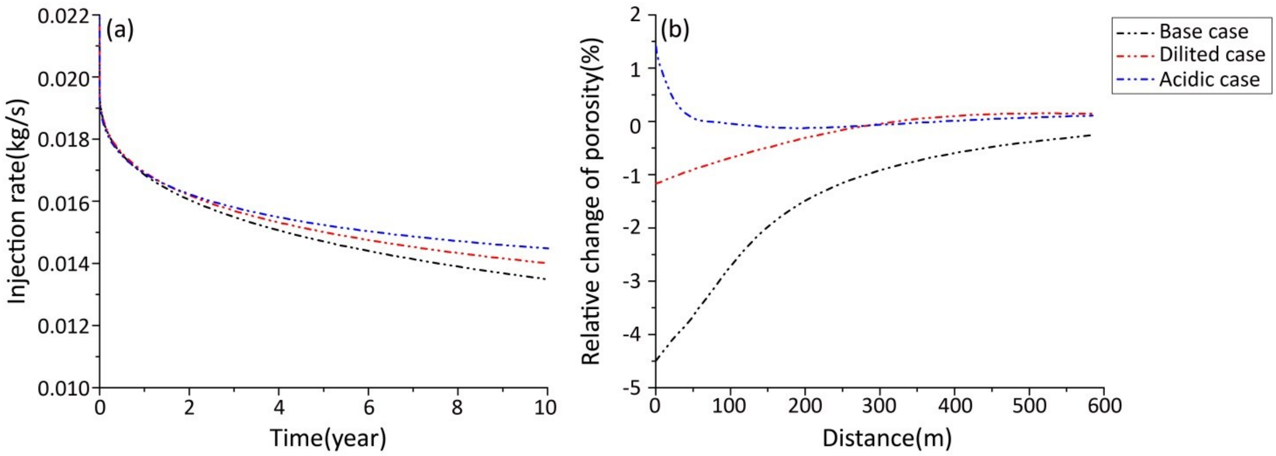

Figure 5: (a) Temporal variation of injection rate over 10 years, and (b) relative change of porosity along the flow path under injection of hydrochemical water, injection of diluted water, and injection of acidic water.

4.3 Simulation of acid injection

The fluid near the injection well after acidification can promote the dissolution of calcite, k-feldspar and illite, following the reaction formula below:

$$CaCO_3 + 2H^+ = Ca^{2+} + H_2O + CO_2 \tag{3}$$

$$K_{0.6}Mg_{0.25}Al_{2.3}Si_{3.5}O_{10}(OH)_2 + 18.6HF + 3.4H^+ = 0.6K^+ + 0.25Mg^{2+} + 2.3AlF_2 + 3.5SiF_4 + 12H_2O \tag{4}$$

$$KAlSi_3O_8 + 14HF + 2H^+ = K^+ + AlF_2 + 3SiF_4 + 8H_2O \tag{5}$$

The reaction rate for the H^+-$CaCO_3$ reaction is extremely high. On the other hand, the surface reaction rates for many mineral reactions are very slow compared with the acid transport rate, and the overall rate of acid consumption and mineral dissolution are controlled by the reaction rate. Quartz, clay and feldspars are the main siliceous particles involved in the reaction process of HF acid. The reaction rates of HF acid with clays and feldspars are approximately two orders of magnitude higher than that between HF acid and quartz. Because the clay and feldspars reaction rates are relatively high and they generally comprise a small portion of the total rock mass, which will be consumed firstly (Fig. 6).

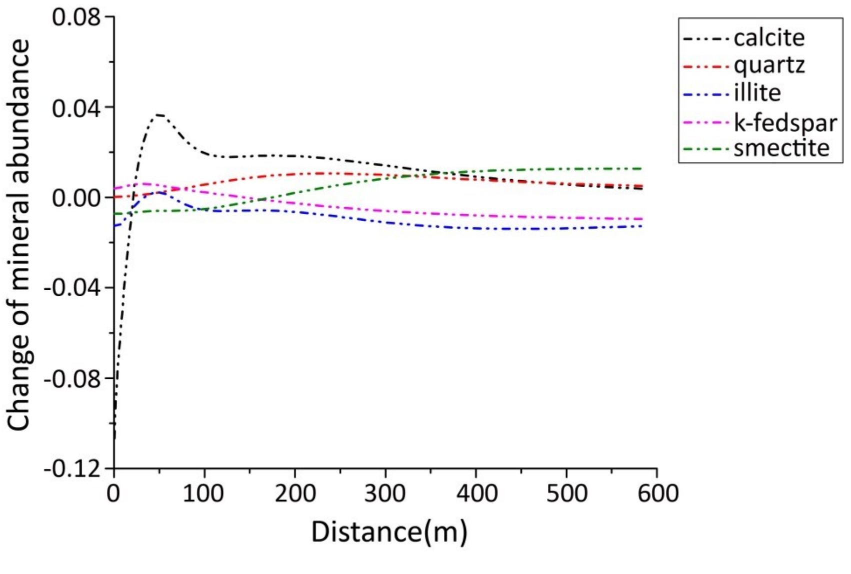

Figure 6: Variation of minerals along the flow path under injection of acidic water.

5. CONCLUSIONS

The circulation of injected cold brine in the 4500-m deep Soultz-sous-forets reservoir was modeled based on simplified 1D model using TOUGHREACT. The fluid flow through the granitic reservoir modifies the chemical and thermal equilibrium in the system, resulting in mineral dissolution and precipitation.

The fluid circulation inside the rock mass is carried out in the hydrothermal altered granite, and the precipitation and dissolution laws of each mineral within 10 years are simulated and analyzed. It was found that calcite is the most reactive mineral, which is consistent with the trend of porosity. Relative porosity decreased by 4.5% near the injection well, mainly due to calcite precipitation. Carbonate dissolution and precipitation control the porosity of the reservoir.

After determining the major scaling minerals, the case of diluted brines and acidified injected water are adopted to prevent and control the scaling. An effective acid treatment method with HF acid at a concentration of 3% is used to enhance the permeability in the reservoir, which can help maintain the long-term productivity of reservoirs in granitic rocks.

6. ACKNOWLEDGEMENT

Funding support for this work is from National Key R&D Program of China (2018YFC0604305-03), and National Natural Science Foundation of China (No. 41572215).

REFERENCES

André, L., V. Rabemanana and F.-D. Vuataz (2005). Geochemical modelling of water-rock interactions and implications on the properties of the Soultz fractured reservoir. Proceedings EHDRA Scientific Conference.

André, L., V. Rabemanana and F. o.-D. Vuataz (2006). "Influence of water–rock interactions on fracture permeability of the deep reservoir at Soultz-sous-Forêts, France." Geothermics **35**(5): 507-531.

André, L., N. Spycher, T. Xu, K. Pruess and F.-D. Vuataz (2008). "Comparing FRACHEM and TOUGHREACT for reactive transport modeling of brine-rock interactions in enhanced geothermal systems (EGS)."

Bächler, D. and T. Kohl (2005). "Coupled thermal–hydraulic–chemical modelling of enhanced geothermal systems." Geophysical Journal International **161**(2): 533-548.

Bear, J. (1972). Dynamics of fluids in porous media.

Dezayes, C., A. Genter and B. Valley (2010). "Structure of the low permeable naturally fractured geothermal reservoir at Soultz." Comptes Rendus Geoscience **342**(7-8): 517-530.

Entingh, D. J. (1999). "A review of geothermal well stimulation experiments in the United States." TRANSACTIONS-GEOTHERMAL RESOURCES COUNCIL: 175-180.

Genter, A., K. Evans, N. Cuenot, D. Fritsch and B. Sanjuan (2010). "Contribution of the exploration of deep crystalline fractured reservoir of Soultz to the knowledge of enhanced geothermal systems (EGS)." Comptes Rendus Geoscience **342**(7-8): 502-516.

Jacquot, E. (2000). Modélisation thermodynamique et cinétique des réactions géochimiques entre fluides de bassin et socle cristallin: application au site expérimental du programme européen de recherche en géothermie profonde (Soultz-sous-Forêts, Bas-Rhin, France), Strasbourg 1.

Kushnir, A. R. L., M. J. Heap and P. Baud (2018). "Assessing the role of fractures on the permeability of the Permo-Triassic sandstones at the Soultz-sous-Forets (France) geothermal site." Geothermics **74**: 181-189.

Lasaga, A. C. (1984). "Chemical Kinetics of Water-Rock Interaction." Journal of Geophysical Research Solid Earth **89**(B6): 4009-4025.

Nitschke, F., J. Scheiber, U. Kramar and T. Neumann (2014). "Formation of alternating layered Ba-Sr-sulfate and Pb-sulfide scaling in the geothermal plant of Soultz-sous-Forets." Neues Jahrbuch Fur Mineralogie-Abhandlungen **191**(2): 145-156.

Portier, N., J. Hinderer, U. Riccardi, G. Ferhat, M. Calvo, Y. Abdelfettah, C. Heimlich and J.-D. Bernard (2018). "Hybrid gravimetry monitoring of Soultz-sous-Forets and Rittershoffen geothermal sites (Alsace, France)." Geothermics **76**: 201-219.

Portier, S. and F. D. Vuataz (2010). "Developing the ability to model acid-rock interactions and mineral dissolution during the RMA stimulation test performed at the Soultz-sous-Forets EGS site, France." Comptes Rendus Geoscience **342**(7-8): 668-675.

Portier, S. and F. o. D. Vuataz "Developing the ability to model acid-rock interactions and mineral dissolution during the RMA stimulation test performed at the Soultz-sous-Forêts EGS site, France."

Tester, J. W., B. J. Anderson, A. S. Batchelor, D. D. Blackwell, R. DiPippo, E. M. Drake, J. Garnish, B. Livesay, M. C. Moore, K. Nichols, S. Petty, M. N. Toksoz, R. W. Veatch, R. Baria, C. Augustine, E. Murphy, P. Negraru and M. Richards (2007). "Impact of enhanced geothermal systems on US energy supply in the twenty-first century." Philosophical Transactions Of the Royal Society a-Mathematical Physical And Engineering Sciences **365**(1853): 1057-1094.

Xu, T. and K. Pruess (2004). "Numerical Simulation of Injectivity Effects of Mineral Scaling and Clay Swelling in a Fractured Geothermal Reservoir." Transactions - Geothermal Resources Council **28**.

Xu, T., N. Spycher, E. Sonnenthal, G. Zhang, L. Zheng and K. Pruess (2011). "TOUGHREACT Version 2.0: A simulator for subsurface reactive transport under non-isothermal multiphase flow conditions." Computers & Geosciences **37**(6): 763-774.